Pergamon

Int. J. Solids Structures Vol. 31, No. 14, pp. 1967–1979, 1994

0020-7683/94 $7.00 + .00

STRESS DISTRIBUTION AND BUCKLING STRESS OF PLATES INCLUDING EDGE CONTACT–FRICTIONAL FORCE EFFECTS

MOHAMMED Z. AHMED and DONALD A. DADEPPO
Department of Civil Engineering and Engineering Mechanics, The University of Arizona, Tucson, AZ 85721, U.S.A.

(*Received* 5 *July* 1992; *in revised form* 28 *September* 1993)

Abstract—The effects of edge contact–frictional force imposed by machine heads on the stress distribution in a plate are investigated. A contact–friction interface element is included in the pre-buckling analysis which considers the possibility of slip between the machine heads and the plate. All analyses are performed using the incremental theory of plasticity. In the buckling formulation of the plate, element stiffness is evaluated on the basis of Hermitian interpolation polynomials. The buckling stresses are compared with those of the test results and the closed-form solutions available in the literature. The effect of edge boundary imperfections is also considered in this paper.

NOTATION

b	width of a plate
$[B]$	strain–displacement matrix
$[C]$	constitutive law matrix
E	modulus of elasticity
E_t	tangent modulus
F^k	Coulomb frictional force
k	load step
$[k]$	element stiffness matrix
$[K]$	structure stiffness matrix
$[K]_b$	bending stiffness matrix of a structure
$[K]_g$	initial stress stiffness matrix of a structure
n	shape parameter of a stress–strain curve
s	initial maximum gap between plate and machine head before loading
t	thickness of a plate
u, v	nodal displacements in global coordinate system
u', v'	nodal displacements in local coordinate system
x, y	global coordinate
x', y'	local coordinate
δ	s/b, a parameter used to measure extent of imperfection
Δ_n	relative normal gap increment between a node pair at interface
Δ_s	relative slip movement increment between a node pair at interface
Δ_n^k	normal gap between a node pair at interface at load step k
Δ_s^k	slip movement between a node pair at interface at load step k
ε	strain
ε_e	effective strain
λ_n	normal interface force for a load increment
λ_s	tangent interface force for a load increment
λ_n^k	normal interface force at load step k
λ_s^k	tangent interface force at load step k
μ	coefficient of friction between machine head and plate
σ	stress
σ_e	effective stress
σ_x	normal stress in transverse direction of a plate
σ_y	normal stress in longitudinal direction of a plate
σ_{xy}	shearing stress
$\sigma_{0.7}$	stress corresponding to a secant of $0.7E$
$\sigma_{0.85}$	stress corresponding to a secant of $0.85E$
ϕ	angle between local and global coordinate.

INTRODUCTION

Recently Gajelsvik and Lin (1987) studied the effect of edge contact–frictional force imposed by machine heads on the plastic buckling stress of plates. In their study it was observed

that plastic buckling stress can be increased if the edge contact–frictional force is eliminated. They considered the plate to be in full contact with the machine head and assumed no-slip (the case "no-slip" means that there is no relative slip movement between the machine head and the edge of the plate) between the machine head and plate. In an attempt to confirm the no-slip assumption they checked that the maximum ratio of shear stress σ_{xy} to normal stress σ_y, i.e. μ at the central Gauss point of the corner elements (boundary) was less than 0.2–0.3, which is the coefficient for friction between aluminium and steel ($\sigma_{xy} \leqslant \mu\sigma_y$). But there is no proof that their confirmation calculation of no-slip really means that no slip occurred at the interface between the edge of the plate and machine head during loading from zero to the buckling load.

In reality, while performing a test for plate buckling, the value of the coefficient of friction between the machine head and plate will depend on the degree of polish of the machine heads and plate edges. In other words, during an actual test, it may happen that some portion of the edge of the plate slips laterally as the plate is compressed by the machine head. In this case, the stress distribution in the plate and the plastic buckling stress will depend upon the values of the friction coefficient between the machine head and the plate. Practically, it can be expected that initially the edges of the plate may not be in full contact with the machine heads at the beginning of loading due to simple edge imperfection.

In this paper the effect of the coefficient of friction, μ, on the stress distribution and the plastic buckling stress of plates is investigated. The possibility of slip between the machine head and the plate is considered. In addition, the effect of edge boundary imperfections on the buckling stress is considered.

ANALYSIS

Stress analysis

The finite element method based on incremental loading is used. In this method, the total load is divided into a series of small load increments such that the stiffness matrix may be treated as being constant within load increments. Four-noded linear two-dimensional isoparametric quadrilateral elements (Cook, 1989) are employed for the stress distribution analysis of the plate. The stiffness matrix of this element is generated according to the following formulation

$$[k] = [B]^T[C][B]t\,\mathrm{d}x\,\mathrm{d}y. \tag{1}$$

Since an incremental form of plasticity is used in this study, the constitutive law matrix $[C]$ based on von Mises' yield criterion and isotropic hardening is included in the element stiffness formulation, which has been generated earlier by Gajelsvik and Lin (1987). The tangent modulus, E_t, as used in matrix $[C]$ is estimated according to the well-known Ramberg–Osgood (1943) stress–strain expression for non-linear materials which is as follows:

$$\varepsilon = \frac{\sigma}{E} + \frac{3}{7}\frac{\sigma}{E}\left(\frac{\sigma}{\sigma_{0.7}}\right)^{n-1}. \tag{2}$$

In eqn (2), n is a shape parameter of the stress-strain curve, which is given by the following equation

$$n = 1 + \frac{\log\left(\frac{17}{7}\right)}{\log\left(\frac{\sigma_{0.7}}{\sigma_{0.85}}\right)}. \tag{3}$$

Upon differentiation, eqn (2) becomes

$$\frac{d\varepsilon}{d\sigma} = \frac{1}{E}\left[1 + \frac{3}{7}n\left(\frac{\sigma}{\sigma_{0.7}}\right)^{n-1}\right]. \tag{4}$$

Thus,

$$E_t = \frac{d\sigma}{d\varepsilon} = \frac{E}{1 + \frac{3}{7}n\left(\frac{\sigma}{\sigma_{0.7}}\right)^{n-1}}, \tag{5}$$

where E_t is the tangent modulus for a uniaxial stress–strain relation. For a multiaxial stress state, using the effective stress and effective strain, E_t (Fig. 1) as obtained from eqn (2) is

$$E_t = \frac{d\sigma_e}{d\varepsilon_e} = \frac{E}{1 + \frac{3}{7}n\left(\frac{\sigma_e}{\sigma_{0.7}}\right)^{n-1}}. \tag{6}$$

For a plane stress problem, the effective stress σ_e in eqn (6) is given by

$$\sigma_e = \sqrt{3J_2} \tag{7}$$

where

$$J_2 = \tfrac{1}{3}(\sigma_x^2 - \sigma_x\sigma_y + \sigma_y^2 + 3\sigma_{xy}^2) \tag{8}$$

is the second invariant of the stress tensor.

To incorporate the effects of edge contact–friction force as imposed by a machine head, the contact–friction interface element formulated by Katona (1983), is adopted in the finite element program. This interface element can account for the three interface states: slip, fixed or free state as may exist at the interface between the edge of a plate and a machine

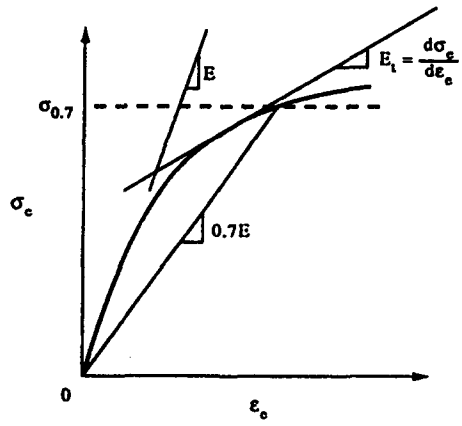

Fig. 1. Typical effective stress–strain curve.

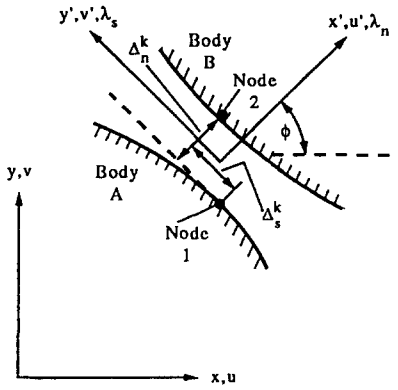

Fig. 2. A contact–friction interface element representation in separated state. [Adapted from Katona (1983).]

head during loading. As shown in Fig. 2, the interface element is defined (Pifko and Isakson, 1969) by two nodes (nodes 1 and 2) and x', y' coordinate system, which makes an angle of ϕ with the global coordinate axes x, y. A dummy node (not shown in Fig. 2) is also included in the interface element formulation to identify the internal forces, λ_n and λ_s, enforcing constraint.

An incremental–iterative algorithm has been given by Katona (1983), which illustrates the implementation and validity of the interface element (Fig. 2). According to this procedure, the solution for the first iteration of the very first load step is determined by assuming that the node pairs of interface elements are in a particular state (fixed, slip, free). This trial solution is then used to determine whether the assumed state is correct and, if not, what new state is to be assumed for the next trial. For example, if the state in a given load step k is assumed fixed, then after the trial solution, it is checked to find if the total normal interface force, λ_n^k (the superscript identifies the load step), is compressive and the total tangent interface force, λ_s^k, is less than the maximum Coulomb frictional force, F^k. If not, the assumed fixed state is incorrect and the new state is slip or free depending on whether the total interface normal force, λ_n^k, is compressive or tensile. Similarly, within an iteration of a given load step k, the assumed slip state is correct if λ_n^k is compressive and the relative slip increment between the node pair (Fig. 2), Δ_s, has the same sign as the Coulomb friction force, F^k. However, if the relative slip increment, Δ_s, has a sign opposite to the friction force, F^k, a fixed state is assumed for the next iteration since the relative slip movement cannot reverse its direction until the passive frictional force reverses its direction. Likewise, an assumed free state is correct if the normal gap, Δ_n^k, is greater than zero. Otherwise, the new state is assumed to be fixed for the next iteration. This also implies that a slip state can be reached from a free state through an iterative path, i.e. free to fixed and fixed to slip. Finally, for a load step the convergence is obtained by satisfying the criterion that the assumed state of each pair of nodes in the interface (the state may be different for different pair of nodes) remains unchanged after the trial solution.

For all the subsequent load steps, the very first iteration starts by assuming the interface state as determined in the step just completed. The solution at the end of load step k is obtained by the following equation

$$\alpha^k = \alpha + \alpha^{k-1} \tag{9}$$

where

$$\alpha^k = \Delta_n^k, \Delta_s^k, \lambda_n^k, \lambda_s^k$$

defines the interface solution at load step k and

$$\alpha = \Delta_n, \Delta_s, \lambda_n, \lambda_s$$

defines the interface solution increments.

Finite element model

The finite element model of the plate, including the machine head, which was used in the stress state investigation, is shown in Fig. 3. The elements of the machine head were considered to be 100 times stiffer than the elements of the plate. In addition, lateral supports are provided in the model (machine head) so that it behaves essentially as a rigid body. This assumption is necessary in order to have the full extent of the effect of friction as imposed by the machine head on the stress distribution in the plate, as well as on the buckling stress of the plate (relative rigidity between the machine head and the plate may have influence on the frictional force effects). As mentioned earlier, an interface element consists of a node pair (node 1 at the machine head and node 2 at the plate as shown in

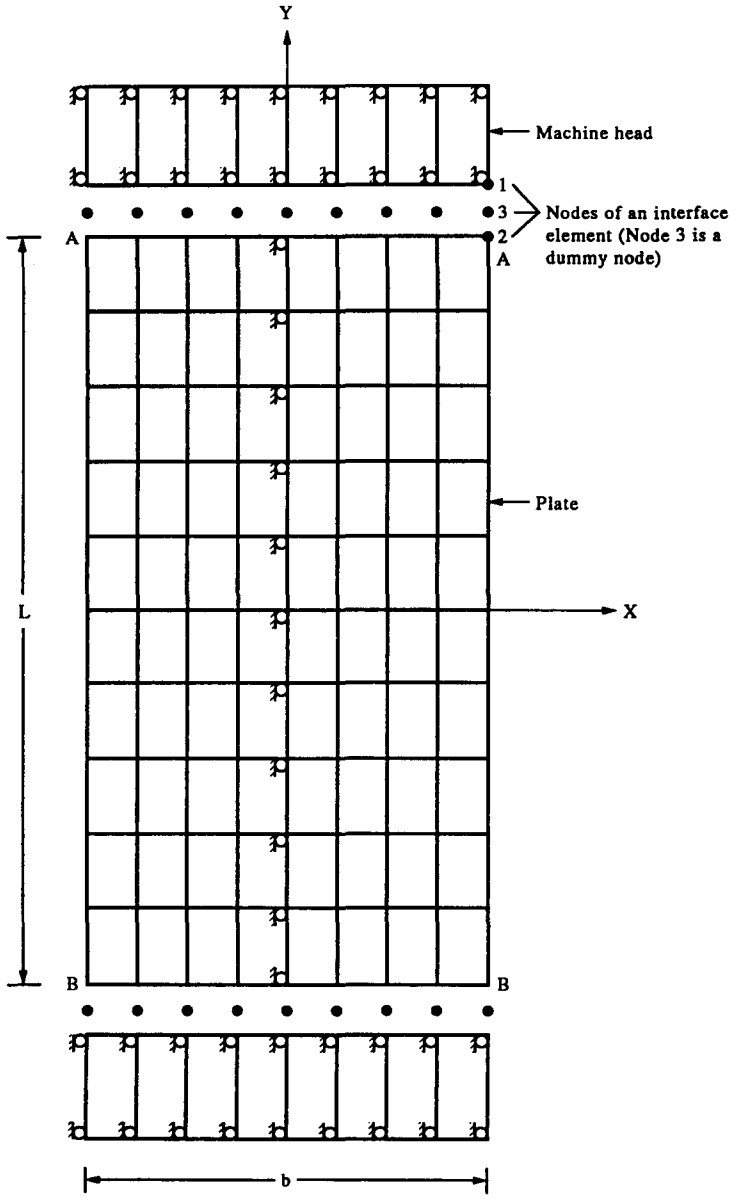

Fig. 3. Finite element mesh for a typical plate including the machine heads.

Fig. 3) and a dummy node (node 3 in Fig. 3). This dummy node is used to identify the unknowns, i.e. the interface normal and tangent force.

Buckling analysis

For the buckling analysis the finite element formulation of plastic buckling of a plate developed by Pifko and Isakson (1969) is employed. This finite element formulation, which was developed originally for the deformation theory of plasticity, is modified for the incremental theory of plasticity using the constitutive law matrix given by Gajelsvik and Lin (1987) for the incremental theory of plasticity. In general, the criterion for buckling of a plate is the vanishing of the determinant of the stiffness matrix $[K]$, written as follows:

$$[K] = [K_g] + [K_m]. \tag{10}$$

Since plastic deformation in the plate is considered, the determinant of $[K]$ is evaluated for each stress state obtained from pre-buckling stress analysis corresponding to each load increment. The unloaded plate is in stable equilibrium, and therefore, initially, $|[K]| > 0$. The transition from stable to unstable equilibrium of the plate is attained when the determinant reduces to zero and the corresponding stress level gives the critical or buckling stress (σ_{cr} = average σ_y over contact edge).

RESULTS

Stress distribution

To study how the cofficient of friction, μ, between the lateral edges AA or BB of the plate and the machine heads (Fig. 3) accounts for the frictional effects in the distribution of stresses, plates were analysed for the values of μ equal to 0.1, 0.2 and 0.7. The plates were considered to be made of 14S-T6 aluminium alloy [the same plate material as used by Pride and Heimerl (1948)]. The values of the Ramberg–Osgood (1943) parameters are taken as $n = 19$, $\sigma_e = 10{,}700$ ksi and $\sigma_{0.7} = 63.2$ ksi for the 14S-T6 aluminium alloy. Uniform incremental displacements were prescribed on the upper edge AA as a stepwise input. The finite element mesh and corresponding stresses (in ksi) at Gauss points along the contact surface are summarized for a typical plate in Fig. 4 to highlight the distribution of stresses at the point of buckling with respect to μ. It is observed that the extent of slippage of the boundary edge AA and BB increases with decreasing values of μ. The distribution of stresses in the elements near the machine head is greatly changed due to different values of μ.

Figure 5 illustrates that the stresses σ_x and σ_{xy} vanish gradually from the edge (near the machine heads) towards the middle of the plate, as expected. Although the stresses σ_x and σ_{xy} along the edge AB on row 2 are zero, they exist in the boundary region. These stresses are dependent on the element size along the y-direction (Fig. 6a). Likewise, due to the variation of the element size along the x-direction, a strong stress gradient is obtained on the corner (Fig. 6b). Thus, the results of these analyses demonstrate that the stress distribution pattern in the plate near the boundary region is dependent upon the degree of friction imposed by the machine heads. On the other hand, the corresponding stress gradient is found to be mesh dependent.

The nature of the stress singularity at the corner elements is also noted (Fig. 4) for the case with no-slip between the rigid machine head and the plate. It may be recalled that the case "no-slip" means that all the pairs of nodes between the machine heads and the edges of the plate remained fixed state and this condition is obtained at $\mu = 0.7$ for the plate problem considered here.

Buckling stresses

To determine the effect of the coefficient of friction, μ, between the machine head and the edge of the plate on buckling stress, plates simply supported on four sides were investigated with different values of μ. In this case the plate is divided into 80 equal size elements (Fig. 3). The buckling stress of a typical plate is presented in Fig. 7. The results indicate that the buckling stress decreases with increasing values of μ. Figure 8 shows the buckling

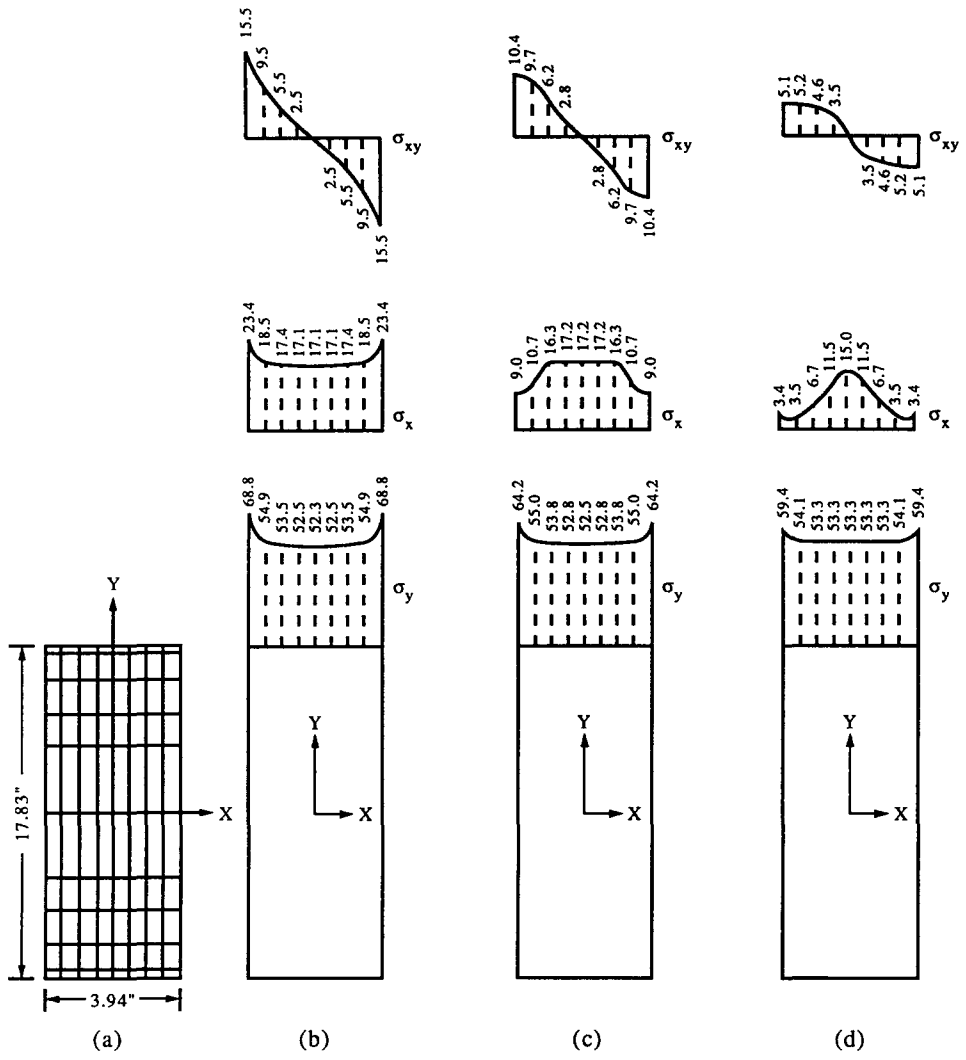

Fig. 4. Stress distribution at the Gauss points along the contact surface at the buckling point for a typical plate. (a) Finite element mesh, (b) $\mu = 0.7$, (c) $\mu = 0.2$, (d) $\mu = 0.1$.

stresses of plates with different width-to-thickness ratio, b/t, for the values of $\mu = 0.7$ (no-slip condition) and 0.0 (frictionless condition). It can be noted that the buckling stress for a typical plate, with $b/t = 25.6$ and $\mu = 0.0$, which is 55.8 ksi, differs from that obtained by Gajelsvik and Lin (1987), where they found it to be equal to 58.34 ksi. This discrepancy between the results is due to the fact that Gajelsvik and Lin did not investigate the buckling stress for the frictionless condition ($\mu = 0.0$) directly by employing the finite element method. Instead, they calculated the buckling stress using the closed-form solution available in the literature. This did not consider the effect of edge frictional force on plate buckling.

In Fig. 8, the buckling stresses obtained are also compared with those obtained by experiments (Pride and Heimerl, 1948) and the closed-form solution using the incremental theory of plasticity (Pearson, 1950). Although the theoretical results are infinitely long plates, these comparisons are still comparable since the lengths taken by Pride and Heimerl were sufficiently large so as to have no effect on buckling stress (usually the buckling stress is not affected when the length-to-width ratio is greater than two). This comparison has shown that the results of this study (FEM) for large frictional coefficients are in better agreement with the experimental results than those based on the closed-form solution. Moreover, it is also observed that due to the effect of edge frictional force (i.e. from frictionless condition to no-slip condition), the buckling stress is reduced marginally from

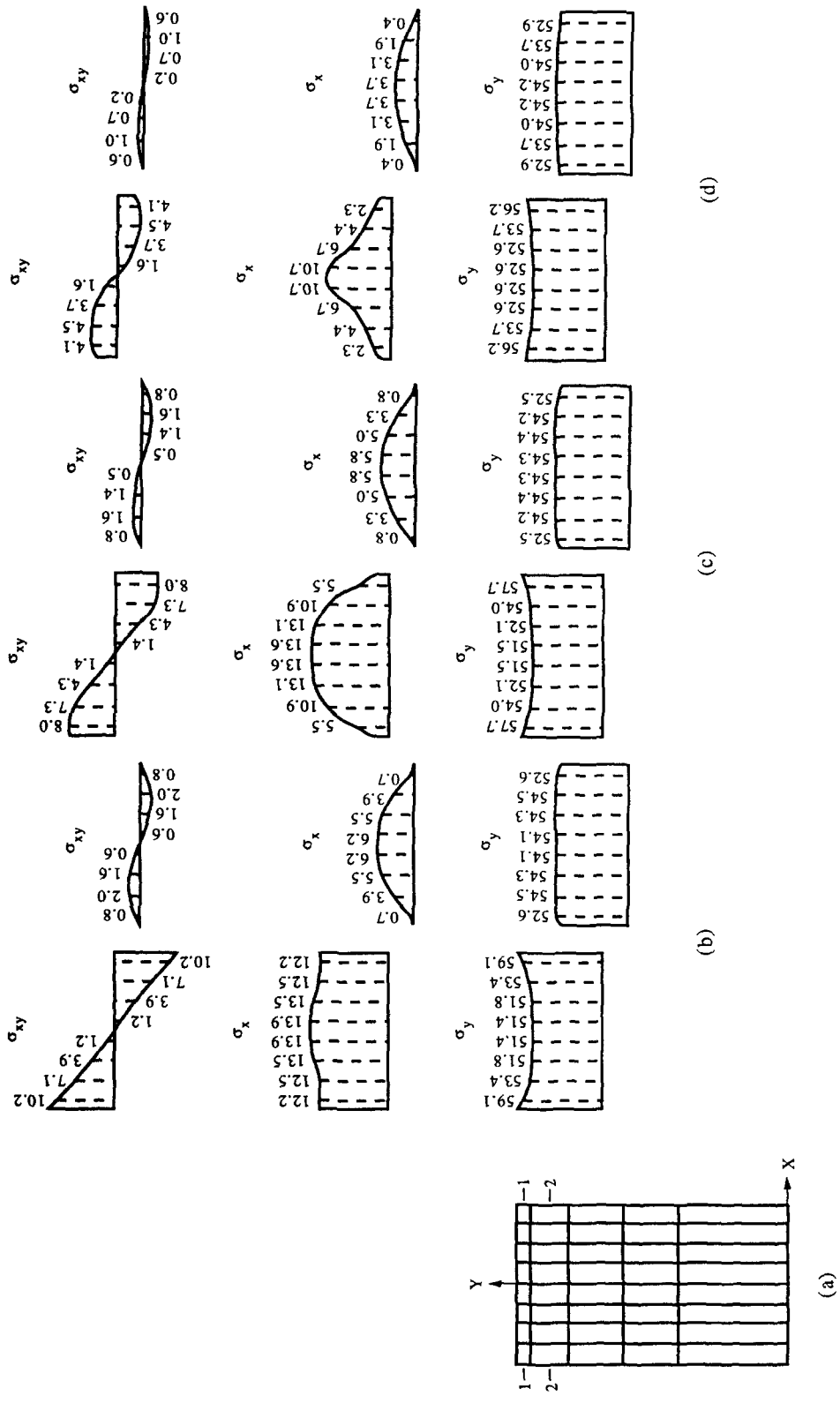

Fig. 5. Stress distribution in the plate along different element levels. (a) $\mu = 0.7$. (b) $\mu = 0.2$. (c) $\mu = 0.1$.

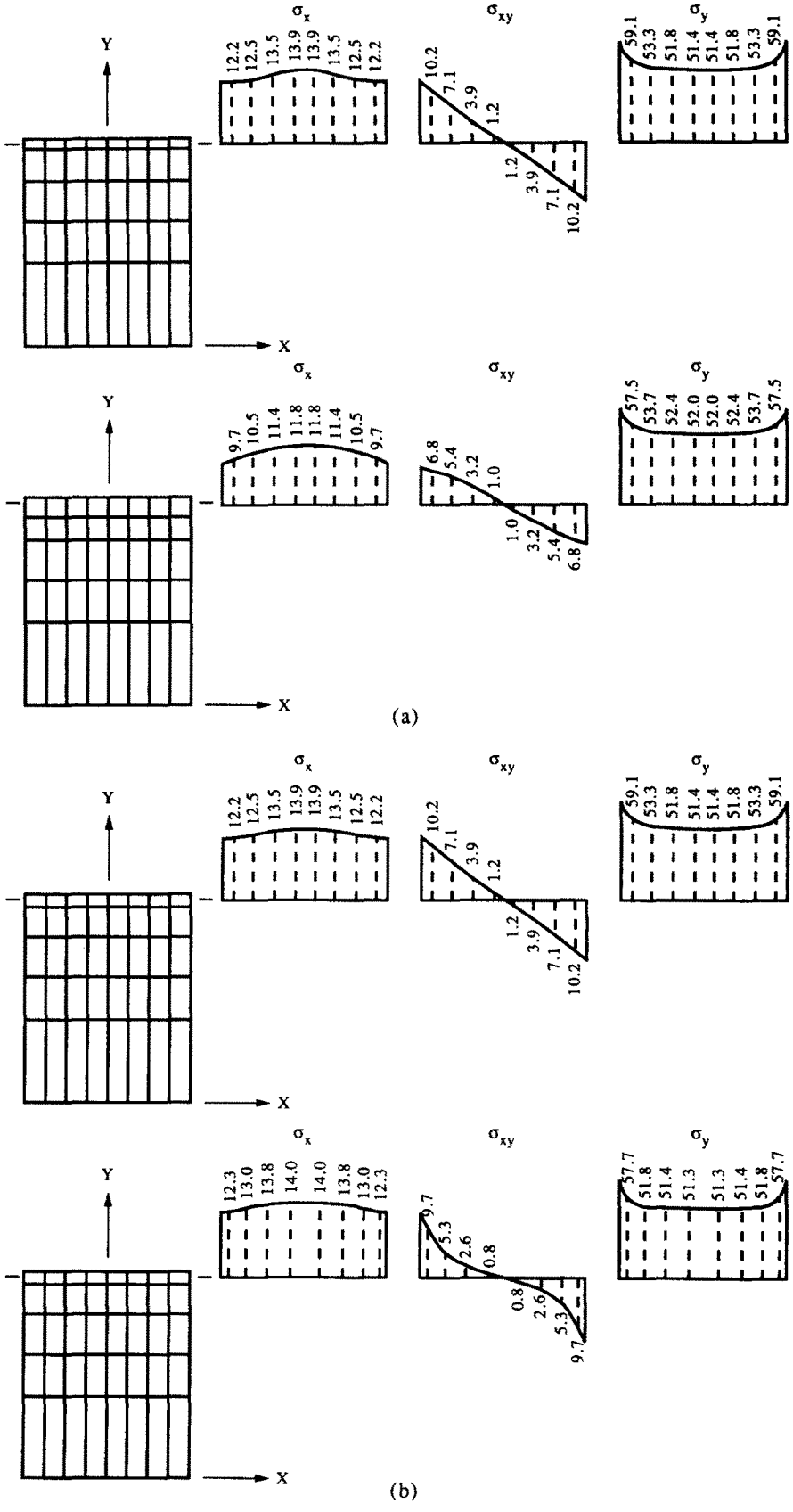

Fig. 6. Stress distribution with respect to element size. (a) Element size along y, (b) element size along x.

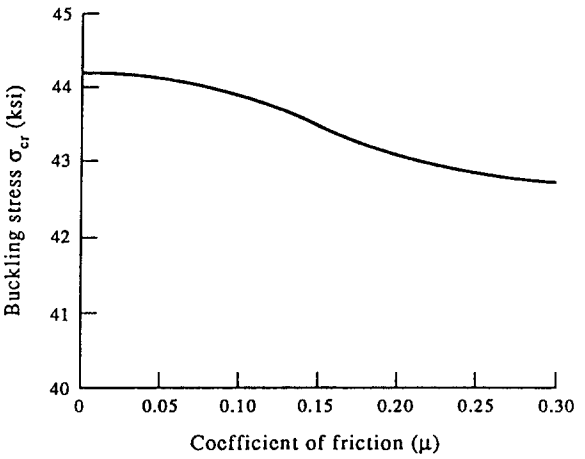

Fig. 7. Buckling stress vs coefficient of friction, μ.

1% to 6% depending on b/t. This decrease in buckling stress is less for a lower width-to-thickness ratio. Thus, the results of the present study contradict those shown by Gajelsvik and Lin (1987). It can be mentioned here that due to the edge friction imposed by the machine heads additional stresses σ_x and σ_{xy} are introduced primarily at the loaded edge boundary of the plate (the region near the machine heads). These stresses may have insignificant effects on reducing the buckling stress of the plate. From this study, it can be concluded that the discrepancy between the test results (Pride and Heimerl, 1948) and the closed-form solution (Pearson, 1950) is not due to the effect of edge contact–frictional force but due to the inadequacy of the particular closed-form solution. In other words, it can be inferred that the particular closed-form solution employed (Pearson, 1950) may not be suitable for buckling stress analysis of a plate for lower values of b/t.

The effect of an edge boundary imperfection on the stress distribution and buckling load has been studied by analysing plates with a convex upper edge as shown in Fig. 9. This case of symmetric imperfection was considered in order to have the advantage of using one half of the plate for pre-buckling and buckling analyses. The convex surface was considered to be parabolic with vertex at the centre of the edge. The lower edge was considered to be perfect. At the beginning of loading, only the centre of the upper edge of the plate was in contact with the machine head. As the load was increased, a line of contact developed and spread from the centre of the plate to the corner points. The magnitude of the imperfection in the plate, as shown in Fig. 9, was expressed by the parameter, $\delta = s/b$,

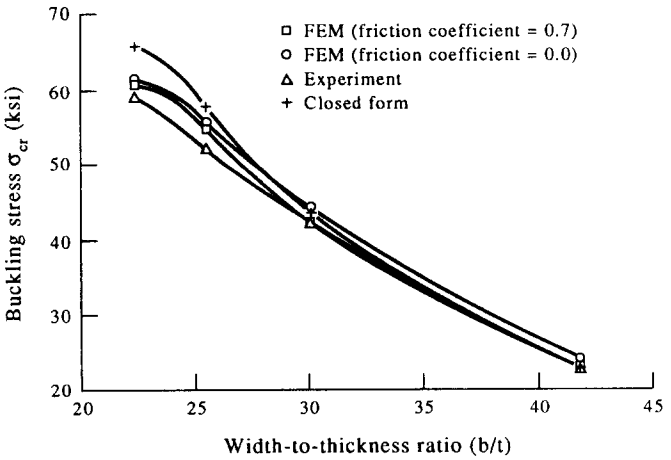

Fig. 8. A comparison of buckling stresses for simply-supported plates.

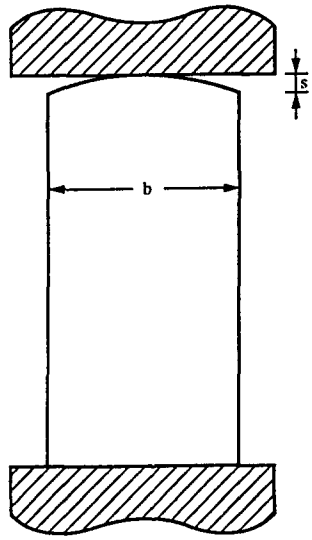

Fig. 9. Plate with edge boundary imperfection (upper edge).

the ratio of the initial maximum gap to the width of the plate. The stress distributions along the boundary elements at the point of buckling for a value of δ equal to 0.002 with $\mu = 0.7$ and 0.0 are presented in Fig. 10 for a typical plate ($b/t = 25.6$). It is observed that σ_y is maximum near the centre of the imperfect edge and decreases gradually towards the corners. A similar distribution is found for stress, σ_x. The distribution of σ_x, σ_y and σ_{xy} near the perfect edge has the same nature as obtained for perfect plates. Although there is no trace of σ_x and σ_{xy} at the edge boundary of the perfect plates for the frictionless condition ($\mu = 0.0$), these stresses exist at the boundary of the imperfect plates. This result demonstrates that additional stresses, i.e. σ_x and σ_{xy}, are introduced in the plate boundary due to imperfection, even if there is no friction between the machine head and imperfect edge of the plate. Several plates were then investigated to determine the critical stresses for different values of the imperfection parameter, δ (as shown in Fig. 11). It is found from Fig. 11 that the buckling stress is reduced significantly due to the imperfection at the loading edge of the plate. This reduction in critical stress is higher for lower width-to-thickness ratios, b/t. It is also noted that the buckling stress of a plate decreases due to imperfection for the case with no-friction between the loading edge and the machine head.

CONCLUSIONS

The effect of edge contact–frictional force imposed by a machine head on the stress distribution and the critical stress of a plate has been demonstrated. Since the possibility of slip between the machine head and the plate has been incorporated, the method presented appears to be a feasible and realistic approach to determine the critical stress of a plate for different values of the coefficient of friction, μ. Based on the analyses performed in this study, the following conclusions can be drawn.

- The actual distribution of stresses in the plate boundary is dependent upon the values of the coefficient of friction.
- The plastic buckling stress of a plate decreases with the increasing values of the coefficient of friction.
- The critical stresses of the plates using the finite element method agree well with the test results.
- The marked disagreement between the results obtained by experiments and the closed-form solution (using the incremental theory of plasticity) is not due to the effect of edge contact–frictional force but due to the inadequacy of the closed-form solution.

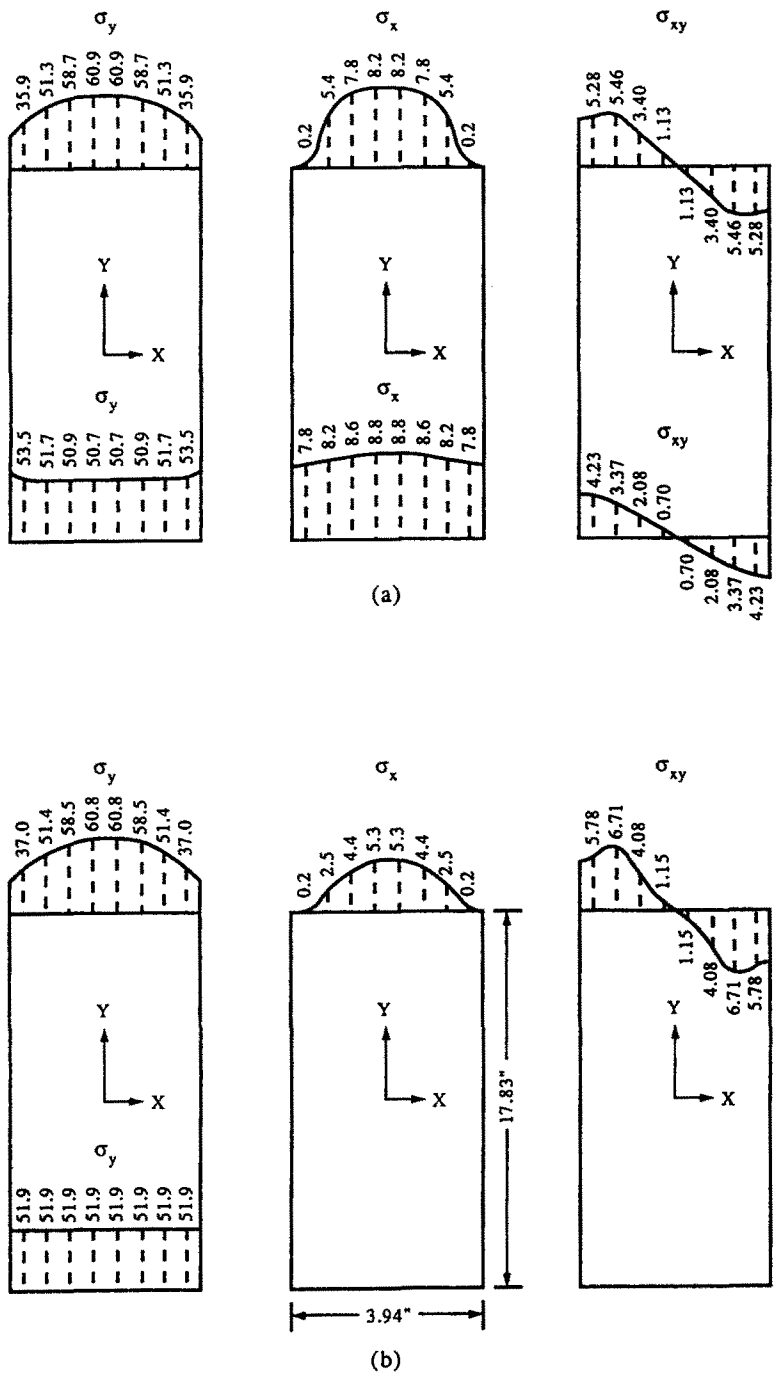

Fig. 10. Stress distribution in the imperfect plate at the buckling point for a typical plate. (a) $\mu = 0.7$, (b) $\mu = 0.0$.

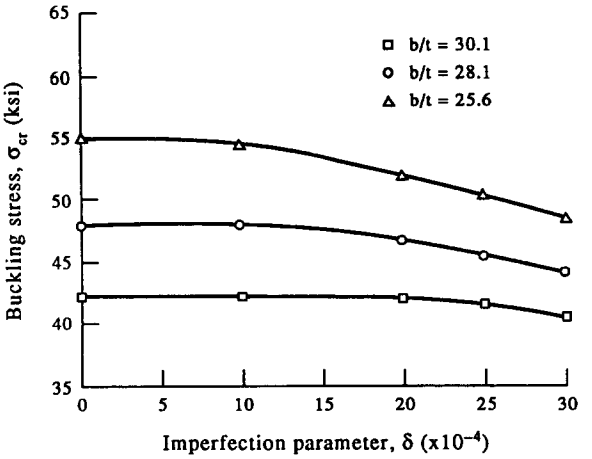

Fig. 11. Buckling stresses for imperfect plates.

- Due to edge imperfection, the critical stress of a plate is reduced. This reduction in critical stress is dependent upon the width-to-thickness ratio and the extent of the edge imperfection.

REFERENCES

Cook, R. D. (1989). *The Concept and Application of Finite Element Analysis*, 2nd edn. John Wiley, New York.

Gajelsvik, A. and Lin, G. S. (1987). Plastic buckling of plates with edge frictional shear effects. *ASCE J. Engng Mech.* **7**, 953–964.

Katona, M. G. (1983). A simple contact–friction interface element with application to buried culverts. *Int. J. Numer. Anal. Meth. Geomech.* **7**, 371–384.

Pearson, C. E. (1950). Bifurcation criterion and plastic buckling of plates and columns. *J. Aerospace Sci.* **7**, 417–424.

Pifko, A. and Isakson, G. (1969). A finite element method for the plastic buckling analysis of plates. *AIAA Jl* **10**, 1950–1956.

Pride, R. A. and Heimerl, G. J. (1948). Plastic buckling of simply supported compressed plates. NACA Technical Note No. 1819.

Ramberg, W. and Osgood, W. R. (1943). Description of stress–strain curves by three parameters. NACA Technical Note No. 902.